United States Department of Commerce
Technology Administration
National Institute of Standards and Technology

NIST Technical Note 1376

Optical Detector Nonlinearity: Simulation

Shao Yang
Igor Vayshenker
Xiaoyu Li
Thomas R. Scott
Mike Zander

Optical Detector Nonlinearity: Simulation

Shao Yang
Igor Vayshenker
Xiaoyu Li
Thomas R. Scott
Mike Zander

Optoelectronics Division
Electronics and Electrical Engineering Laboratory
National Institute of Standards and Technology
325 Broadway
Boulder, Colorado 80303-3328

May 1995

U.S. DEPARTMENT OF COMMERCE, Ronald H. Brown, Secretary
TECHNOLOGY ADMINISTRATION, Mary L. Good, Under Secretary for Technology
NATIONAL INSTITUTE OF STANDARDS AND TECHNOLOGY, Arati Prabhakar, Director

National Institute of Standards and Technology Technical Note
Natl. Inst. Stand. Technol., Tech. Note 1376, 40 pages (May 1995)
CODEN:NTNOEF

U.S. GOVERNMENT PRINTING OFFICE
WASHINGTON: 1995

For sale by the Superintendent of Documents, U.S. Government Printing Office, Washington, DC 20402-9325

CONTENTS

Optical Detector Nonlinearity: Simulation

Shao Yang*, Igor Vayshenker, Xiaoyu Li, and Thomas R. Scott
National Institute of Standards and Technology
Optoelectronic Division
Boulder, Colorado 80303

W. Michael Zander
Army Primary Standards Laboratory
USATA
Redstone Arsenal, Alabama

Abstract

We have developed a unified mathematical treatment for five commonly used methods of measuring optical detector nonlinearity. We performed computer simulations to compare these methods for different measurement conditions and data processing options. The triplet and differential methods gave the best overall results, and third- and fourth-order polynomial representations of the measurement results will yield the least total error for a common practical measurement system.

Keywords: nonlinearity, optical power calibration, optical detector, simulation

*Shao Yang is with Ohmeda Medical Systems, Inc., Louisville, Colorado 80027

1. Introduction

Optical detector linearity has always been an important issue for people who are concerned about the accuracy of an optical radiation measurement. The calibration of an optical power meter from a characterized optical power transfer standard is often performed at one power. To extend the calibration to the full dynamic range of the power meter, it is essential to measure the meter linearity. Even when a power meter is used for relative measurements such as attenuation measurements of a large magnitude, the knowledge of the meter nonlinearity will improve the measurement accuracy. Many laboratories have studied the problem of detector linearity and have developed various methods to measure this property. Each method has advantages and disadvantages relative to their resulting accuracy, precision, and effectiveness. However, we found it difficult to choose a best method suitable for optical power meters by simply comparing the published results. This was due to the fact that each of the previous individual efforts used their own method of analysis, and results were reported with expressions using different definitions of detector nonlinearity; it was, therefore, impossible to make a direct comparison of these published results. The purpose of this work is to investigate theoretically some of the major issues that have an impact on the accurate measurement of detector nonlinearity. These issues are related to definition, measurement methods, data uncertainties, and data processing.

It is important to adopt a single definition and use a unified mathematical treatment to describe the nonlinearity of a detector measured by different methods. Only then can we compare these methods on a common basis. For this purpose, we employed a specific definition of detector nonlinearity and derived useful expressions based on this definition for data processing and comparison of different methods. These mathematical expressions and derivations are presented in section 2 of this paper. Section 3 describes, in terms of the basic expressions laid out in section 2, the five methods we considered. These are the methods now most commonly used by various laboratories. We also derived relationships between the definitions used by the different laboratories.

The comparison study was done using computer simulations. Section 4 describes how the simulations were performed and gives results of the simulations. The computer simulations studied issues common to the five methods, such as effects due to type and magnitude of data error, number of data points, and the order of the curve-fitting polynomial. For this analysis, all five methods were compared under the same conditions. Where appropriate, issues specific to individual methods were also studied in the simulations. We found that the quality of results produced by these methods is significantly affected by the characteristics of the detector being studied. Also, the choice of polynomial order used for data processing has a substantial effect on the systematic error and random uncertainty of the results, and, thus, there is an optimum polynomial order for each specific condition. The results of the simulations helped us to choose the method, the design of measurement system, and the optimum data processing to achieve a desired accuracy.

To measure optical radiation, a detector always needs accompanying equipment such as electronic circuits and display instruments. It is not always possible to separate the detector from these elements, so we characterized not just the detector, but the detection system. Because the underlying principle is the same whether we measure the nonlinearity of a single detector or a detection system, we will simply use the word 'detector' in the remainder of this paper.

2. Definition and Basic Expressions

2.1. Definition

In the Draft International Standard of Calibration of Optical Power Meters [1], a document of the International Electrotechnical Commission (IEC), nonlinearity is defined as "Departure from linear response, i.e., the difference between the response at an arbitrary power level and the response at the reference power level, divided by the response at the reference power level." The reference power is usually the calibration power P_c. This definition can be expressed as

$$\Delta_{NL}(P;P_c) = \frac{R(P) - R(P_c)}{R(P_c)}, \tag{1}$$

where $R(P) = V/P$ is the responsivity of the detector at optical power P incident on the detector, the subscript c indicates calibration, and V is the detector output, which can be electric current or voltage, or the display reading from a power meter. The relationship between the detector output and the input power is described by the response function

$$V = V(P). \tag{2}$$

The responsivity R(P) can thus be written as

$$R(P) = \frac{V(P)}{P}. \tag{3}$$

Using eq (3), we express the nonlinearity of eq (1) in terms of the response function:

$$\Delta_{NL}(P;P_c) = \frac{V(P)P_c}{V(P_c)P} - 1. \tag{4}$$

Because the purpose of measuring the detector nonlinearity is to estimate the accuracy of or to make corrections to optical radiation measurements, nonlinearity of

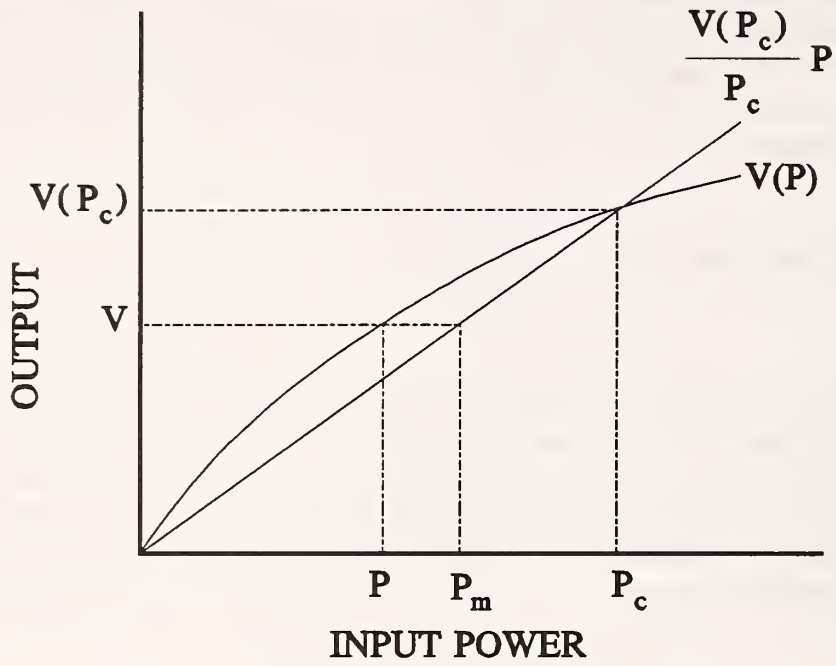

Figure 1. Response function.

eq (1) can equivalently be expressed as the error it causes in the measurement of optical power:

$$\Delta_{NL} \equiv \frac{P_m - P}{P}, \tag{5}$$

where $P_m = V/R(P_c) = V(P)P_c/V(P_c)$ is the measured optical power, which is dependent on calibration as is illustrated in the response curve of a detector in figure 1. Once the detector nonlinearity is measured, a correction can be made to obtain the actual power P from the measured power P_m:

$$P = \frac{P_m}{1 + \Delta_{NL}} \approx P_m(1 - \Delta_{NL}). \tag{6}$$

The approximate equality in eq (6) holds because Δ_{NL} is usually very small (no more than a few percent) and the higher order terms can be ignored in the Taylor series expansion of $(1 + \Delta_{NL})^{-1}$.

The inverse of the response function is called the conversion function, illustrated in figure 2, which converts the output V to the input power P and is written as

$$P = P(V). \tag{7}$$

In the real measurement, it is more convenient to use the conversion function than the response function. Equation (7) may be used in eq (1) to express nonlinearity Δ_{NL} in terms of V and the conversion function:

$$\Delta_{NL}(V;V_c) = \frac{P(V_c)V}{P(V)V_c} - 1. \tag{8}$$

There are two types of nonlinearity. The first is the saturation type, where the responsivity R(V) decreases with increasing input power P, or output V. The second type is called supralinearity [2], where the responsivity increases with the input power, or the output. The two types of nonlinearity can therefore be distinguished by the sign of the first derivative of the responsivity dR(P)/dP or, from eq (1), by the sign of the first derivative

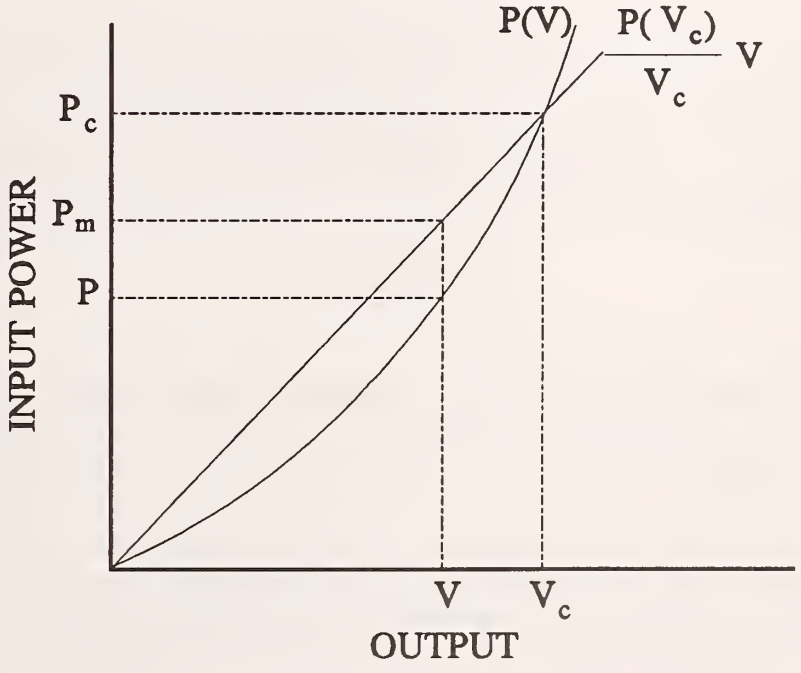

Figure 2. Conversion function.

of nonlinearity $\Delta_{NL}(P;P_c)$ or $\Delta_{NL}(V;V_c)$:

$$\frac{d\Delta_{NL}(V;V_c)}{dV} < 0 \qquad \text{saturation type;}$$
$$\frac{d\Delta_{NL}(V;V_c)}{dV} > 0 \qquad \text{supralinear type.} \tag{9}$$

It is often necessary to characterize the nonlinearity of a detector before calibrating it. However, the definition of nonlinearity Δ_{NL} is referred to the calibration power P_c (or calibration output V_c). Since the output V is directly measurable while the power P is derived from V through calibration, using nonlinearity expressions in terms of V makes it possible to characterize the nonlinearity of a detector without calibration. We can use a dummy calibration output, or reference output, V_r for the expression of nonlinearity $\Delta_{NL}(V;V_r)$. If later the detector is calibrated at power P_c where the output is V_c, the detector nonlinearity referred to V_c can simply be calculated from the nonlinearity referred to V_r through the relation

$$\Delta_{NL}(V;V_c) = \Delta_{NL}(V;V_r) - \Delta_{NL}(V_c;V_r). \tag{10}$$

Again this relation holds with the assumption that nonlinearity is very small. Since V_r is not a real calibration point, it can be 0, representing a limiting case:

$$\begin{aligned}\Delta_{NL}(V;0) &= \lim_{V_r \to 0}[\Delta_{NL}(V;V_r)] \\ &= \frac{P'(0)V}{P(V)} - 1,\end{aligned} \tag{11}$$

where $P'(0)$ is the derivative of the conversion function $P(V)$ at $V=0$.

2.2. Polynomial Expression

We now have all the basic expressions for characterizing the nonlinearity of a detector. But we still need a specific form of the conversion function (or response function) to really do so. Because the conversion function cannot generally be expressed in a closed form, a polynomial is frequently used to represent it [3,4]:

$$P(V) = \sum_{k=1}^{n} a_k V^k. \tag{12}$$

When the nonlinearity is small, a polynomial can represent the conversion function well.

The responses of the commonly used photodiodes, Si, Ge, or InGaAs, are exponential with respect to input power, but they are often used in nearly short-circuited or reverse-biased configurations to achieve a more linear response. As a result, their response can be approximated as a polynomial produced by Taylor series expansion shown in eq (12), where the zero-order term is not included because we assume that the dark output of the detector is always adjusted to 0. If the dark output is not 0, we can add a zero-order term in the polynomial.

The nonlinearity Δ_{NL} of eq (8) now becomes

$$\Delta_{NL}(V;V_c) = -\sum_{k=2}^{n} \frac{a_k}{a_1}(V^{k-1} - V_c^{k-1}) \tag{13}$$

when the nonlinearity is very small.

The factor a_k/a_1 in eq (13) suggests that we can further simplify the polynomial expression by dividing all the coefficients a_k by the first coefficient a_1 without altering the nonlinearity Δ_{NL}. The polynomial thus obtained is called normalized polynomial and is denoted by p(V):

$$p(V) = V + \sum_{k=2}^{n} b_k V^k, \tag{14}$$

where $b_k = a_k/a_1$. The normalized conversion function p(V) can be turned to the general conversion function P(V) through the determination of the coefficient a_1 by means of calibration. If the calibration power is P_c and its corresponding output is V_c, we have

$$a_1 = \frac{P_c}{p(V_c)}. \tag{15}$$

Equation (15) holds for conversion functions P(V) and p(V) in general. P(V) is the calibrated conversion function, p(V) the uncalibrated conversion function, and a_1 the calibration factor or correction factor (fig. 3). In terms of the normalized polynomial, eq (13) becomes

$$\Delta_{NL}(V;V_c) = -\sum_{k=2}^{n} b_k(V^{k-1} - V_c^{k-1}). \tag{16}$$

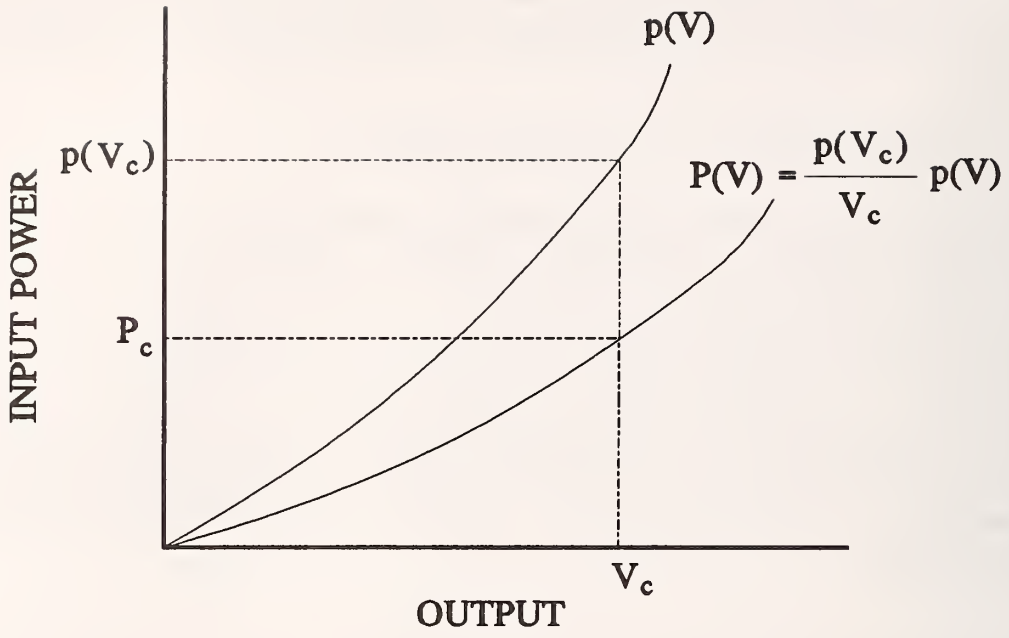

Figure 3. Calibrated and uncalibrated conversion functions.

3. Measurement Methods

Methods for the measurement of detector nonlinearity can be divided into two groups: dependent and independent measurements. Dependent methods always involve the known values or the measurement of some physical quantities other than the output of the detector under test. Typical methods in this category are the inverse square-law method [5], Bouguer's law method [5], Beer's law method [5], and the attenuation method [3,6]. Independent methods rely solely on the measurement of the output of the device under test. The superposition (addition) method and the differential method belong to this group. We favor independent methods over dependent methods since they are more direct. Three variations of the superposition method, the differential method, and the attenuation method from the dependent group are considered in this study. The attenuation method is probably the only dependent method still being used. This is because of the simplicity of the setup and, perhaps, because the other quantity involved in this method is an optical parameter, the transmittance of an optical filter. The attenuation method can also be handled as an independent method if the transmittance of the filter is treated as an unknown parameter in the data processing. Both the dependent and independent

treatments of the attenuation method are studied in this work.

3.1. Superposition Method

The superposition method uses two types of systems: beam superposition [3,4,7-10] and aperture superposition [11-14]. Figures 4 and 5 depict these two systems. The beam superposition method, shown in figure 4 uses a single light source with a beam splitter to get two beams from the source and then the two beams are recombined on device under test (DUT). Precautions must be taken to avoid interference between the two combined beams in this design. A more recent design is an optical fiber system which includes optical fiber attenuators, couplers, and splitters. There are many designs of apertures used in the aperture superposition method, which is mainly used for the integral-step superposition method.

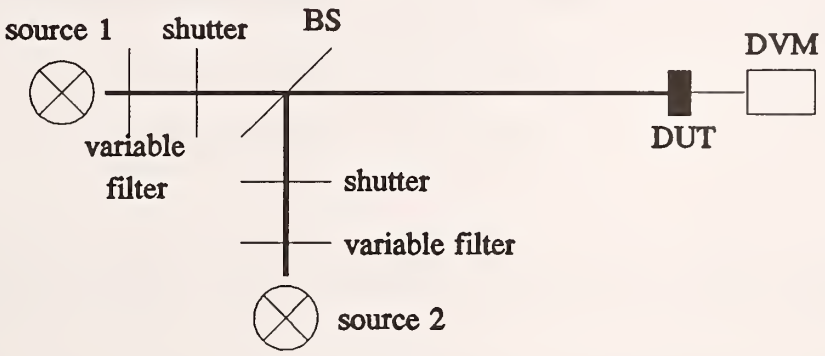

Figure 4. Beam superposition method.

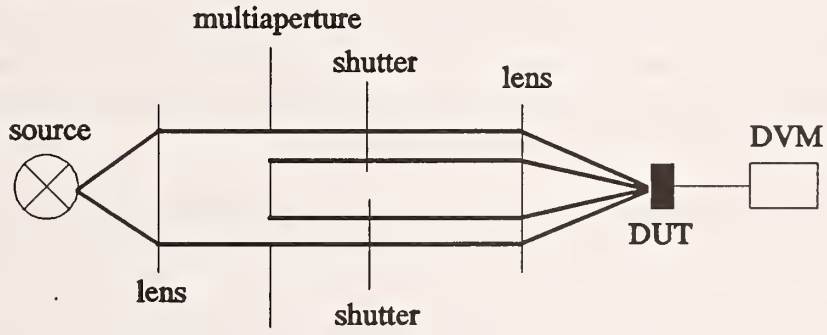

Figure 5. Aperture superposition method.

3.1.1. Integral-Step Superposition Method

The power from one of the two beams, Beam 1, is adjusted to an arbitrary power P_1, which is usually at the lower end of the measurement range, when the other beam, Beam 2, is blocked [7,8]. The corresponding output from the detector is V_1. Then Beam 1 is blocked, and Beam 2 is opened and adjusted so that the detector output is exactly V_1, which indicates that the incident power from Beam 2 is also P_1. Then both beams are opened and combined. The power incident onto the detector is $2P_i$. The detector output is recorded as V_2. V_2 may not equal $2V_1$ because of detector nonlinearity. Repeating the superposition steps, we can get any integral multiples of the power unit P_1 and their corresponding outputs of the detector. This is illustrated in Table I.

Table 1. Illustration of integral-step superposition.

Beam 1	Beam 2	Beam 1 + Beam 2
$P_1 \Rightarrow V_1$	$V_1 \Rightarrow P_1$	$P_1 + P_1 = 2P_1 \Rightarrow V_2$
$V_1 \Rightarrow P_1$	$V_2 \Rightarrow 2P_1$	$P_1 + 2P_1 = 3P_1 \Rightarrow V_3$
:	:	:

With n measurements made, we obtain n sets of data (j, V_j), where j is power in integers of an arbitrary unit. When n is sufficiently large, an uncalibrated conversion curve in the form of normalized polynomial can be obtained by linear least-squares curve fitting.

A second definition of nonlinearity can also be used with integral-step superposition measurement [9-14]. When this definition is used, the powers from the two individual beams in every step are always adjusted the same and equal to the combined power of the previous step. Thus the powers, individual or combined, are always in powers of 2 of the initial arbitrary unit power, as illustrated in table 2.

If we define the nonlinearity as NL, then for measurements as shown on the first line of table 2:

Table 2. Illustration of integral-step superposition.

Beam 1	Beam 2	Beam 1 + Beam 2
$P_1 \Rightarrow V_1$	$V_1 \Rightarrow P_1$	$P_1 + P_1 = 2P_1 \Rightarrow V_2$
$V_2 \Rightarrow 2P_1$	$V_2 \Rightarrow 2P_1$	$2P_1 + 2P_1 = 4P_1 \Rightarrow V_4$
$V_4 \Rightarrow 4P_1$	$V_4 \Rightarrow 4P_1$	$4P_1 + 4P_1 = 8P_1 \Rightarrow V_8$
:	:	:

$$NL = \frac{(V_1 + V_1) - V_2}{V_2} = \frac{2V(P_1)}{V(2P_1)} - 1. \tag{17}$$

Similar expressions hold for measurements at other powers. Using eq (5) and switching from expressions in terms of P to expressions in terms of V, we obtain the following relation between NL and Δ_{NL}:

$$NL = \frac{\Delta_{NL}(V_{11};V_c) - \Delta_{NL}(V_1;V_c)}{1 - \Delta_{NL}(V_1;V_c)} \approx \Delta_{NL}(V_{11};V_c) - \Delta_{NL}(V_1;V_c) = \Delta_{NL}(V_{11};V_1) = \Delta_{NL}(2P_1;P_1). \tag{18}$$

This result indicates that the nonlinearity NL is, indeed, the nonlinearity Δ_{NL} at the combined beam power with reference to the individual beam power.

Integral-step superposition is straightforward. The data sets are pairs of power and output, and the powers are integral multiples of an arbitrary unit. However, the integral multiples of the power are judged by reading the detector output. Therefore the accuracy of those multiples cannot be higher than that of the output V. In addition, uncertainies in the powers of the earlier steps will be carried to later steps and hence there is an accumulation of uncertainty.

3.1.2. Modified Superposition Method

In the modified superposition method [4] the input powers from the two beams vary arbitrarily and the outputs are recorded. Using the normalized conversion polynomial, we have, for the ith measurement of a single beam:

$$P_i = V_i + \sum_{k=2}^{n} b_k V_i^k, \tag{19}$$

where the P_i are arbitrary unknowns and the V_i are their corresponding measured outputs. Because for each measurement we have one unknown power, there are always more unknowns than equations, and the coefficients of the polynomial can never be determined from the measurement data. However, when we use superposition of all combinations of the individual measurements from the two beams, we will get new equations without increasing the number of unknowns:

$$P_i + P_j = V_{ij} + \sum_{k=2}^{n} b_k V_{ij}^k, \tag{20}$$

where subscripts i denotes the ith power from beam 1, j the jth power from beam 2, and ij their combination. If we have m individual measurements from beam 1 and n measurements from beam 2, we will have m × n combinations of new measurements and m × n new equations with no new unknowns. When enough measurements are made, there will be more equations than unknowns, and the coefficients b_k can be obtained by linear least-squares fitting.

Although data points in approximately equal increments of power are preferred, no exact increments are required. This is a big improvement over the integral-step method because it will greatly ease the measurement process and eliminate some sources of uncertainty.

3.1.3. Triplet Superposition Method

In the triplet superposition method [3], a group of three measurements is made, two for individual powers from each beam and one for the combination of the two. Then the powers of the two individual beams are varied arbitrarily and combined again. For the ith group of measurements, we have a set of three equations:

$$\begin{cases} P_{1i} = V_{1i} + \sum_{k=2}^{n} b_k V_{1i}^k, \\ P_{2i} = V_{2i} + \sum_{k=2}^{n} b_k V_{2i}^k, \\ P_{1i} + P_{2i} = V_{3i} + \sum_{k=2}^{n} b_k V_{3i}^k, \end{cases} \tag{21}$$

where the P_i are arbitrary unknowns and the V_i are measured output values. A new equation

$$(V_{3i} - V_{1i} - V_{2i}) + \sum_{k=2}^{n} b_k (V_{3i}^k - V_{1i}^k - V_{2i}^k) = 0 \tag{22}$$

is formed by eliminating the unknown P_i in the group of the three equations eq (21). Again the coefficients b_k can be obtained by linear least-squares fitting when enough data sets have been measured.

There are many similarities between the modified superposition and the triplet superposition methods. Data taken for the modified superposition method can also be arranged in groups of triple measurements if data for individual beams are used several times in different groups. Then they can be processed the same way as the triplet method. Likewise, data taken in the triplet method can be processed as data taken in the modified superposition method by keeping the powers as unknowns. However, the two measurement procedures are different in one respect. In the triplet measurement, the three measurements in one group are usually made in immediate succession. In the modified superposition method, because all combinations of individual power from the two beams are needed, it is not always possible to make all the individual and combined measurements in immediate succession. The triplet procedure reduces the uncertainty that might occur due to the slow drift of the output of the light source. If a fixed pattern of measurements is used, this source drift will cause some systematic error in the measurement for the modified superposition method. One means to reduce this error is to reverse the measurement procedure and use the average value of the forward and backward measurements for each datum. Another way is to randomize the steps of the measurement of individual and combined powers and thus convert this drift error to a random uncertainty and further reduce it by increasing the number of data points taken. The two procedures of taking data and of data processing can therefore be combined in four ways, and we may choose any one of them. We considered two different methods for the triplet method in our study.

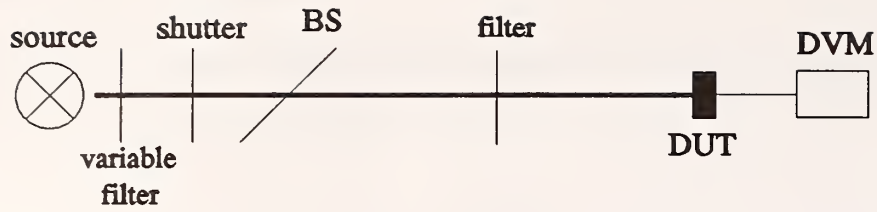

Figure 6. Attenuation method.

3.2. Attenuation Method

Figure 6 shows a schematic of the attenuation method [3]. Ideally, the filter has a fixed density that is constant over the entire measurement power range. It is inserted in the optical path at different powers, and the outputs of the attenuated and unattenuated beams are measured. Expressing the ith measurement in the normalized conversion polynomial, we have

$$\begin{cases} P_i = V_i + \sum_{k=2}^{n} b_k V_i^k, \\ \tau P_i = V_{\tau i} + \sum_{k=2}^{n} b_k V_{\tau i}^k, \end{cases} \tag{23}$$

where τ is the transmittance of the neutral density filter, and $V_{\tau i}$ and V_i are measured outputs with and without the filter. The unknown P_i is eliminated by forming the equation

$$(V_{\tau i} - \tau V_i) + \sum_{k=2}^{n} b_k (V_{\tau i}^k - \tau V_i^k) = 0. \tag{24}$$

The coefficients b_k can be obtained by linear least-squares fitting.

The fitting results rely on the value of transmittance τ being used. It is in general a measured quantity and therefore has uncertainty. This is an extra source of uncertainty specific to this method. The common way of measuring the transmittance is similar to this attenuation method described above. The magnitude of τ is obtained by

$$\tau = \frac{V_\tau}{V}. \tag{25}$$

The transmittance τ in eq (25) is indeed an approximate value of τ measured at power P and biased by detector nonlinearity. We can further express eq (25) as

$$\tau(P) = \frac{V_\tau}{V} = \frac{V(\tau P)}{V(P)} = \tau \frac{V(\tau P)P}{V(P)\tau P}. \tag{26}$$

Then, using eq (4), we have

$$\begin{aligned} \tau(V) = \frac{V_\tau}{V} &= \tau[1 + \Delta_{NL}(\tau P;P)] \\ &= \tau[1 - \Delta_{NL}(V;V_\tau)]. \end{aligned} \tag{27}$$

Because $\lim_{V\to 0}(V_\tau) = 0$ and $\lim_{V\to 0}[\Delta_{NL}(V;0)] = 0$, the true value of τ is the value when the output V is 0, or the input power P is 0:

$$\lim_{P\to 0}\left(\frac{V_\tau}{V}\right) = \lim_{V\to 0}\left(\frac{V_\tau}{V}\right) = \tau. \tag{28}$$

Using eq (16) in eq (27), we obtain for polynomial expression

$$\begin{aligned} \left(\frac{V_\tau}{V}\right) &= \tau[1 + \sum_{k=2}^{n} b_k(V^{k-1} - V_\tau^{k-1})] \\ &= \tau + \sum_{k=1}^{n-1} c_k(V^k - V_\tau^k), \end{aligned} \tag{29}$$

where τ and c_k are unknowns to be determined by curve fitting. τ is the zero-order term of this polynomial. The coefficients b_k of the normalized conversion polynomial are obtained by $b_k = c_{k-1}/\tau$. Thus τ and the conversion polynomial are obtained at the same time from the measurement. This approach of the attenuation method falls in the independent category, where the prior knowledge of the transmittance τ is not necessary.

Nonlinearity measured by the attenuation method is sometimes expressed as the percent change of the transmittance measured at output V or input power P with respect to the transmittance measured at a reference output V_r or input power P_r:

$$NL = \frac{\tau(V) - \tau(V_r)}{\tau(V_r)}. \tag{30}$$

Using eq (27), we can relate this nonlinearity NL to the nonlinearity Δ_{NL} as

$$NL \approx -[\Delta_{NL}(V;V_\tau) - \Delta_{NL}(V_r;V_{r\tau})], \tag{31}$$

where again it is assumed that the nonlinearity is very small so its higher-order terms can be ignored. If τ is unknown and if $V=P^\alpha$, where α is a constant, then the attenuation method should not be used, because $V_\tau/V=\tau^\alpha$.

The most attractive feature of the attenuation method is that it needs only one light source and thus simplifies the measurement setup.

3.3. Differential Method

A schematic diagram of the measurement [15] is shown in figure 7. Figure 8 is an illustration of the method by means of the conversion curve. A small constant ac power ΔP is superimposed onto a varying dc power P. A dc meter and an ac meter are used to measure the ac output $h(V) = k\Delta V(V)$ at different dc output V, where k is used because different meters are used for dc and ac readings. Because ΔP is constant, $h(V) \propto \Delta V(V)/\Delta P$. When ΔP is sufficiently small, we have

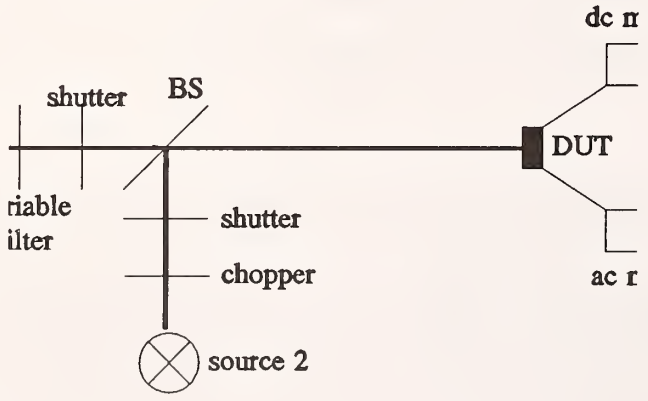

Figure 7. Differential method.

$$\lim_{\Delta P \to 0} \frac{\Delta V}{\Delta P} = \frac{1}{dP(V)/dV}. \tag{32}$$

h(V) is then approximately proportional to the reciprocal of the derivative of the conversion curve at V:

$$h(V) = k\Delta V \approx \frac{k\Delta P}{dP(V)/dV} = \frac{\alpha}{dP(V)/dV}, \tag{33}$$

where $\alpha = k\Delta P$. The conversion curve is obtained by integrating the reciprocal of h(V):

$$P(V) = \int_0^V \frac{dP(V')}{dV'} dV' = \int_0^V \frac{\alpha}{h(V')} dV', \tag{34}$$

where V′ is a dummy variable.

When polynomial expressions are used, we first obtain a polynomial for the reciprocal of h(V) by curve fitting:

$$\frac{1}{h(V)} = \sum_{k=0}^{n-1} c_k V^k. \tag{35}$$

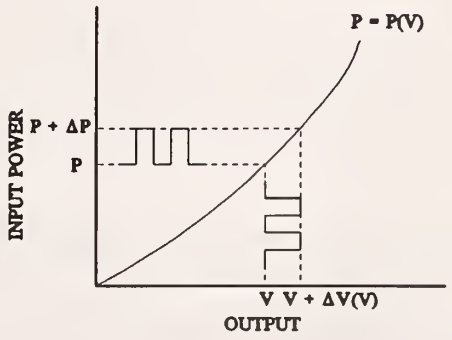

Figure 8. Differential method.

Then we obtain the conversion polynomial by integration:

$$P(V) = \int_0^V \alpha \sum_{k=0}^{n-1} c_k V'^k dV' = \sum_{k=1}^{n} a_k V^k, \tag{36}$$

where $a_k = \alpha c_{k-1}/k$. Dividing every term by a_1, we obtain the normalized conversion polynomial with coefficients $b_k = a_k/a_1 = c_{k-1}/kc_0$:

$$p(V) = V + \sum_{k=2}^{n} b_k V^k. \tag{37}$$

This calculation is based on the assumption that the intensity of the input ac signal is constant during the measurement, which ensures that $\alpha = K\Delta P$ is constant. In a real measurement, however, this assumption does not always hold, and α is not constant. Error will be introduced if we still treat α as a constant. In order to reduce the effect of source intensity drift, a modified procedure of taking and processing the data is used. Immediately after each h(V) is measured, the dc signal is blocked and the ac output at 0 dc input is measured. Because any ac light signal has a dc component, the dc output is not 0 when the dc signal is blocked. It is the dc component V_0 of the ac output. Thus the ac output measured is $h(V_0)$ when dc is blocked. The ratio of $h(V_0)/h(V)$ is then taken; that is,

$$\frac{h(V_0)}{h(V)} = \frac{dP(V)/dV}{dP(V)/dV|_{V=V_0}}. \tag{38}$$

The conversion function is then

$$P(V) = \int_0^V \frac{dP(V)}{dV}\bigg|_{V=V_0} \frac{h(V_0)}{h(V')} dV'. \tag{39}$$

Comparing this equation with eq (34), we see that the factor $\left.\frac{dP(V)}{dV}\right|_{V=V_0}$ has replaced α.

Because this factor is a function of the dc component V_0 of the ac output, it still varies with the changing intensity of the input ac. However, we will show in Appendix that the effect of ac drift on this factor is much less than that on α.

The ac input power cannot be made very small due to considerations of signal-to-noise ratio and the lowest range of the ac meter. Thus, the measured h(V) does not represent the true derivative of the conversion curve; thus an error will result. This problem is also studied by computer simulation and presented in the next chapter.

4. Computer Simulation

The purpose of this study is to consider what variations the experiment and data processing will affect the final result. We will consider five different methods, two kinds of data uncertainties at three different levels, and four different polynomial orders. It is not always possible to vary some of the conditions deliberately on a particular measurement system, whereas any situation can be simulated on the computer. Nevertheless, not everything can be studied by the simulation, especially systematic errors due to a specific measurement setup. Our study is limited to the effects of random data uncertainty, systematic error due to the truncating of polynomials, their combined effect, and their effect on the different methods. We also studied issues specific to some individual methods, such as the accuracy of the transmittance τ obtained from the attenuation measurement and the effect of finite ac power input for the differential method.

The simulations were performed in the following way. We assumed a polynomial of finite order as an original response curve. A real conversion curve would need a polynomial of infinite order to represent it. The inverse function of an arbitrary polynomial of finite order is generally a polynomial of infinite order. In this sense, the conversion function, which is the inverse of our assumed response function, resembles the conversion function of a real detector and we can study the error due to the omitting of higher order terms. Because we knew the exact response function, the exact nonlinearity Δ_{NL} was known and used to calculate the error in the result.

From the assumed response polynomial, we created data of incident powers and their corresponding outputs for different methods. The power covers a range of one order of magnitude. The data were then processed in the way described in the previous chapter for each method, and conversion polynomials of orders from 2 to 5 were obtained. The resultant curve does not coincide with the original curve. The difference is the systematic error (we know it exactly, so it is not an uncertainty) due to the truncation of the polynomial and may also be due to some specific technical problems related with individual method, for example, the finite input power in the differential method.

We then introduced random uncertainties with chosen standard deviation into the output data. The random uncertainties have a Gaussian distribution. For the integral-step superposition method, accumulated uncertainties were also added to the integers representing powers. We then processed the data thus created to obtain the conversion curves. Next we calculated the nonlinearities from the fitted curve and from the original response curve. The difference between the two calculated values is the error caused by both the truncation of the polynomial and the random uncertainty of the data.

This process was repeated 50 times for each case and standard deviation σ of the nonlinearity difference was calculated:

$$\sigma = \left[\frac{1}{50}\sum_{j=1}^{50}(\Delta_{NLj} - \Delta_{NL})^2\right]^{\frac{1}{2}}, \tag{40}$$

where Δ_{NL} is the original nonlinearity and Δ_{NLj} is the resultant nonlinearity of the jth measurement. If we denote the average nonlinearity of the 50 measurements as $\bar{\Delta}_{NL}$, we can further express the standard deviation σ as

$$\sigma = \left[(\bar{\Delta}_{NL} - \Delta_{NL})^2 + \frac{1}{50}\sum_{j=1}^{50}(\Delta_{NLj} - \bar{\Delta}_{NL})^2\right]^{\frac{1}{2}}. \tag{41}$$

This shows that σ is actually a combination of the systematic error and the random uncertainty. The first term represents the systematic error due to truncation of the polynomial, and the second term is the standard deviation caused by data random uncertainty. We call σ total uncertainty or combined uncertainty.

Three types of data random uncertainties represent different measurement conditions. The first is when all the data in the same output range of the measurement have the same absolute standard deviation. This is the case when the uncertainty is due to the least count of the digital meter or detector dark current noise. Over one decade of the input power, the relative uncertainty of the data varies by one order of magnitude. The second type is where all the data have equal relative standard deviation. A typical example is noise due to source intensity fluctuation. The third type is uncertainty due to shot noise. In this case, the uncertainty is proportional to the square root of the power. Our simulation considers the first two cases only because the magnitude of the uncertainty in the third case lies somewhere between the first two cases.

4.1. Results

Results are presented in figures 9 through 21 that follow. When different methods are compared on the same plot, SI stands for integral-step superposition method, SM for modified superposition method, ST for triplet superposition method, AT-1 for attenuation method with known transmittance, AT-2 for attenuation method with unknown transmittance, and DF for differential method. The response functions we assumed in the simulations are listed in table 3. The percentages in table 3 are nonlinearities calculated at P = 1 with a dummy calibration power at 0. These percentages are used as indicators of these functions when they appear in the same plot. When only one response function is used, it is always the first function listed above. Data are created between P = 0.1 and

Table 3. Assumed response function used in the simulation.

3%:	$V = 2P + 0.05P^2 + 0.008P^3 + 0.002P^4$
1%:	$V = P - 0.03P^2 + 0.05P^3 - 0.01P^4$
0.5%:	$V = P + 0.013P^2 - 0.002P^3 - 0.006P^4$
0.15%:	$V = 2P + 0.005P^2 - 0.003P^3 + 0.001P^4$

P = 1. The dummy calibration power is always 0 unless otherwise stated. The transmittance is 0.5 for the attenuation method.

4.1.1. Systematic Error

Figure 9 shows the systematic error due to truncation of the polynomial for the methods considered. All the methods show the same trend, that the systematic error is less when higher-order polynomial is used. The three superposition methods and the attenuation method with known transmittance τ have almost the same systematic error, while the differential method and the attenuation method without known τ have larger errors. That the differential method has a larger error is due to the fact that for the same polynomial order of the final conversion function to be compared with other methods, we are actually fitting the derivative of the conversion polynomial which has one less order than the conversion polynomial, as is indicated by eq (35). As for the attenuation method with unknown τ, eq (29) shows that all the coefficients b_k are affected by the fitted value of τ, the zero-order term in the fitting polynomial, from which the final conversion polynomial is obtained by dividing each coefficient by τ. We noticed that each fitting parameter usually has a higher error than that of the complete curve. The larger error in τ caused the larger error in the conversion curve of this method than those in the other methods.

Because Figure 9 was obtained for one particular response curve that we have assumed, one may ask whether it is representative for any response curve. To answer this question, we conducted the same simulation with four different response curves (see table 3), each having a different nonlinearity. The result for the integral-step method is shown in figure 10, from which we can draw the following conclusions. The magnitude of systematic error due to truncation of the fitting polynomial is different for different response functions. Although the main trend remains the same, the slope from one order of polynomial to the next can be quite different, which depends on the relative significance of each term in the conversion polynomial.

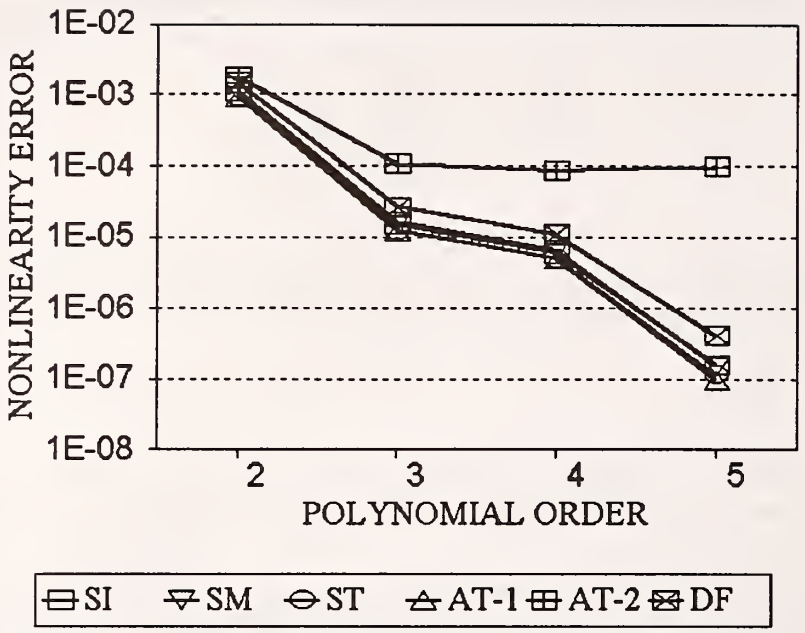

Figure 9. Systematic error due to polynomial truncation.

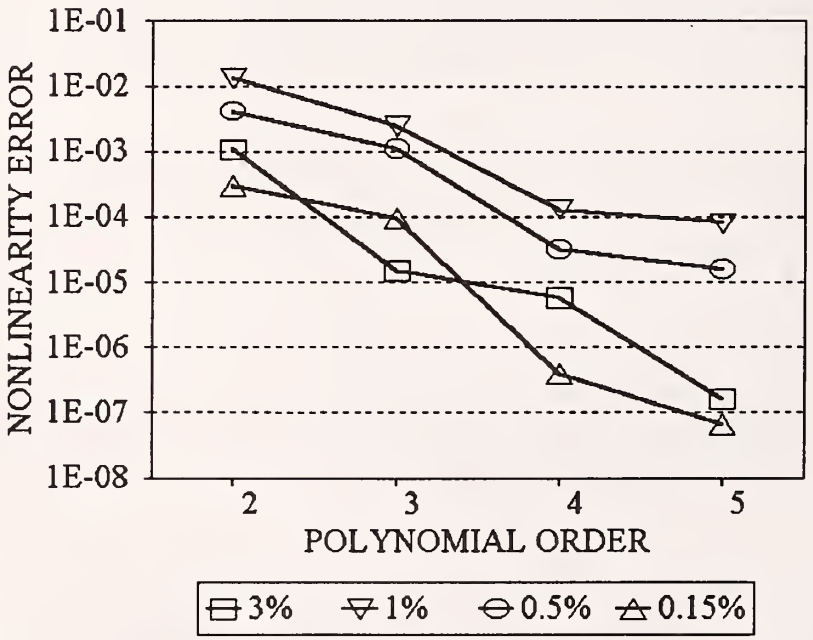

Figure 10. Systematic error of integral-step superposition method for the four different response polynomials listed in table 3.

4.1.2. Random Uncertainty

The effect of random data uncertainty is demonstrated in figure 11. First we notice that all the curves are the same, that is, uncertainty of the result increases with increasing number of order of fitting polynomial. The sign of the slope is opposite to that induced by systematic error. The reason is that the lower-order polynomial has less freedom in fitting. It represents the general shape of the conversion curve more than the details of the curve. It is therefore less influenced by any single data point. As a result, lower-order polynomials are less affected by the random uncertainties of the data and thus yield results with lower deviations.

The attenuation method with unknown transmittance τ and the integral-step superposition method yield significantly larger uncertainties than all the other methods, and the differential method gives the least uncertainty. In the attenuation method, τ is one of the fitting parameters, and it is more sensitive to the data random uncertainty than the entire fitting curve. The larger random uncertainty of τ is then carried into all the b_k through eq (29). The final conversion curve, which is constructed from all the b_k, bears a higher uncertainty than those directly obtained from the fitting for other methods. In the case of the integral-step superposition method, the high standard deviation is due to the fact that there are random uncertainties in both measured variables, the output V and the input power, and the random uncertainty accumulates as the power increases.

The differential method yields the least random uncertainty of all because the fitting curve, which is the derivative of the conversion curve, has one less polynomial order than the fitting curves of the other methods, which are the conversion curves. For this reason, the differential method has a higher standard deviation. If, in figure 11, we move the curve for the differential method horizontally to the left a distance of one polynomial order, it will almost overlap with the curves representing the superposition methods and the attenuation method with known τ. This suggests that the cause of the lower uncertainty of this method is that the fitting polynomial in this method has actually one less order than the final conversion polynomial, which is obtained directly from fitting in other methods.

The differential method also has two independent variables, DC output V and AC output h(V). However, the uncertainty due to V is much less than that due to h(V) if the two variables have the same relative uncertainties. Simulations of this method are presented in figure 12.

4.1.3. Combined Uncertainty

When we consider the systematic error and random uncertainty at the same time, we have the combined uncertainty σ of eq (41), demonstrated in figure 13. Because the systematic error and the random uncertainty behave differently with respect to polynomial order, there is an optimum polynomial order where the combined uncertainty is minimum. In the case shown in figure 13, the optimum is the third order. For polynomial orders higher than this optimum one, the random uncertainty is higher than the systematic error,

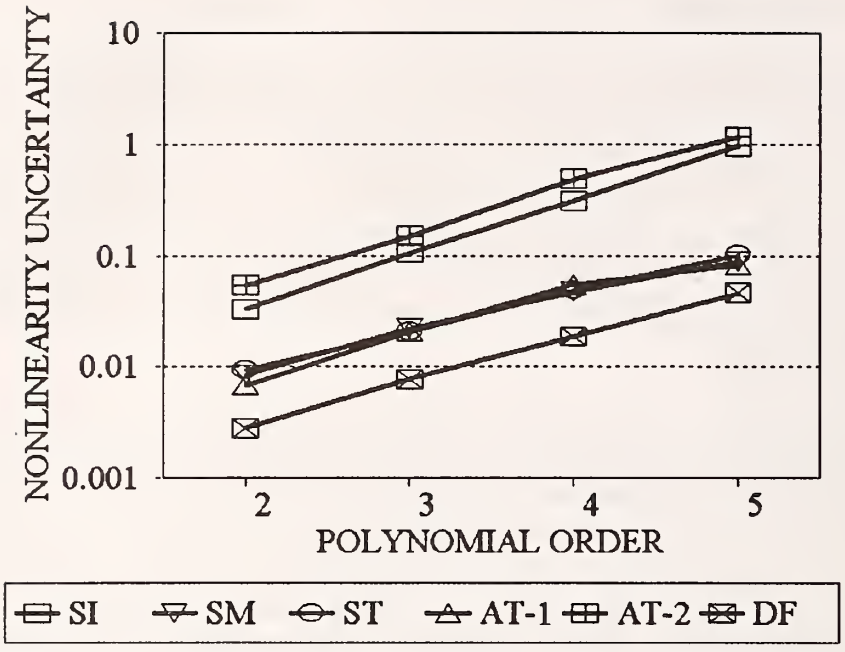

Figure 11. Nonlinearity uncertainty due to data random uncertainty. The data have an equal absolute random uncertainty which is 1 percent of the value at the middle of the range.

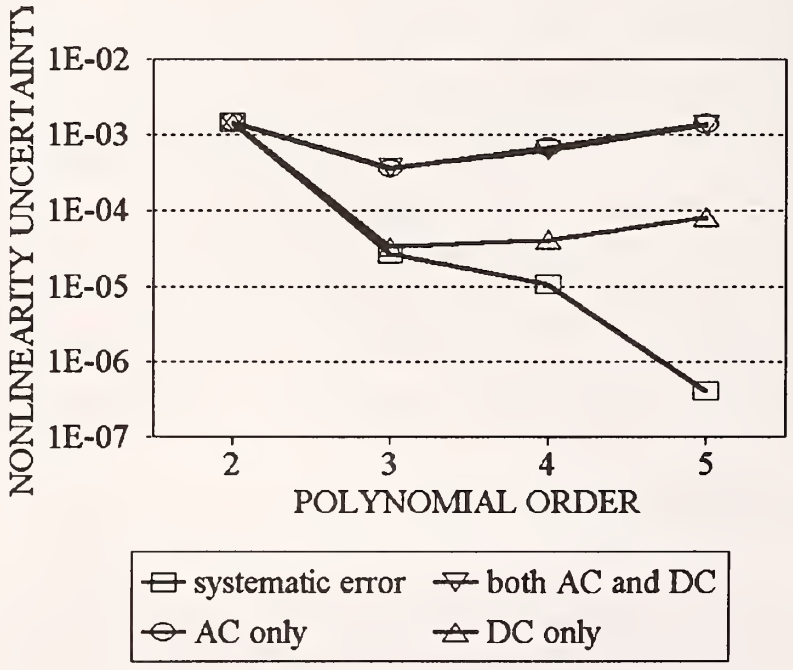

Figure 12. Differential method nonlinearity uncertainty due to data random uncertainty in ac or dc or both, compared to systematic error.

and the combined uncertainty behaves the same as random uncertainty, while for the lower orders, the systematic error dominates and the combined uncertainty behaves the same as systematic error.

The systematic error, the random uncertainty, and the combined uncertainty are demonstrated in a different way in figure 14, where curves for different data uncertainties are presented for the attenuation method. When the data uncertainty is highest, systematic error is always lower than random uncertainty for all the polynomial orders shown. When data uncertainty decreases, the random uncertainty falls until at the second order it is almost the same as systematic error. Further reducing the random uncertainty of the data makes the combined uncertainty determined by systematic error at second order and by random uncertainty at higher orders; therefore, the total uncertainty is minimized at the third-order polynomial.

In figure 15, four curves representing combined uncertainties for four different response functions with different nonlinearity uncertainty are depicted. These are the same four situations represented in figure 10. Figure 15 shows that the behavior of the random uncertainty does not rely on the form of the response function. Therefore, the conclusions about the behavior of the random uncertainty can be applied to any real detectors, even if they do not have similar response functions. But when systematic error dominates, as in the second order and third order, the results differ significantly for the four cases. Since combined uncertainty can never be made lower than the systematic error, we suggest using polynomials whose systematic error is well below the desired uncertainty and using other techniques, such as data averaging, to further reduce the random uncertainty.

Figures 11 through 15 are for data uncertainty of equal absolute uncertainty. Figure 16 is the combined uncertainty when the data have an equal relative uncertainty of 0.01 percent. It shows the same behavior as the case of the equal absolute uncertainty shown in figure 13. However, if we look carefully at the scales, we see that equal relative uncertainty yields a lower combined uncertainty than the equal absolute uncertainty when the latter has the same relative uncertainty at the mid-range. At the lower end of the range, data of equal relative uncertainty have lower relative uncertainty than data of equal absolute uncertainty. We are considering nonlinearity $\Delta_{NL}(V;0)$ whose reference linear curve is the tangent of the conversion curve at 0, which is primarily determined by the behavior of the lower end of the conversion curve. Higher relative uncertainty at the lower end thus will result in higher deviation of the reference linear curve, which in turn worsens the overall uncertainty of the nonlinearity.

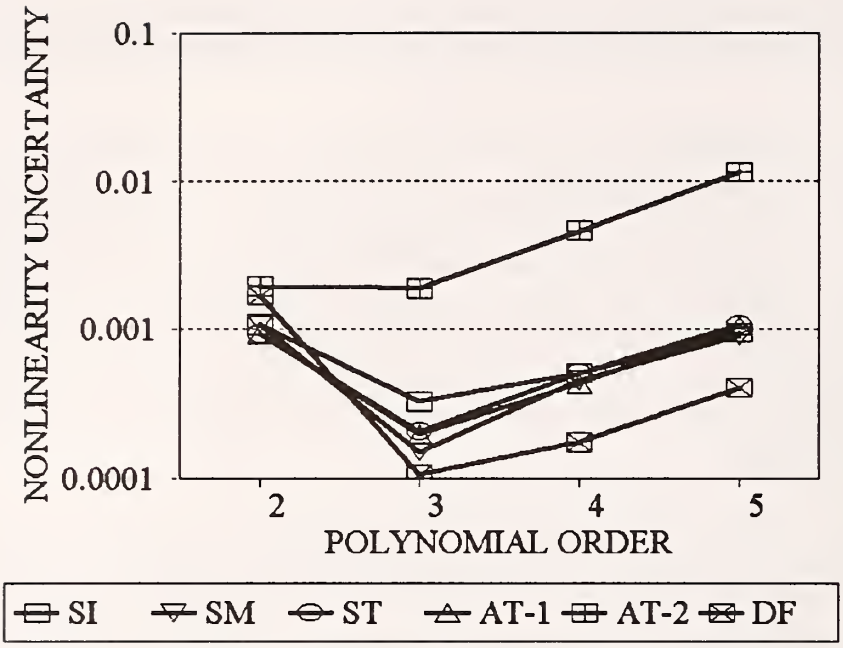

Figure 13. Combined nonlinearity uncertainty. The data have an equal absolute uncertainty which is 0.1 percent of the data value in the middle of the range. The third-order polynomial gives the least combined uncertainty.

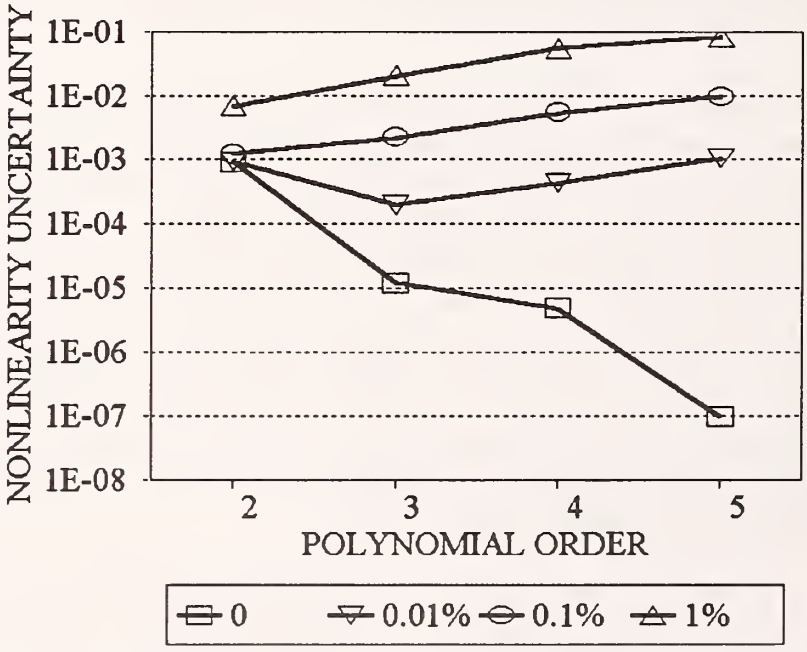

Figure 14. Nonlinearity uncertainty for attenuation method with known transmittance when data have random uncertainty and is dominated by random error for high polynomial order. It is limited by systematic error for the low polynomial orders.

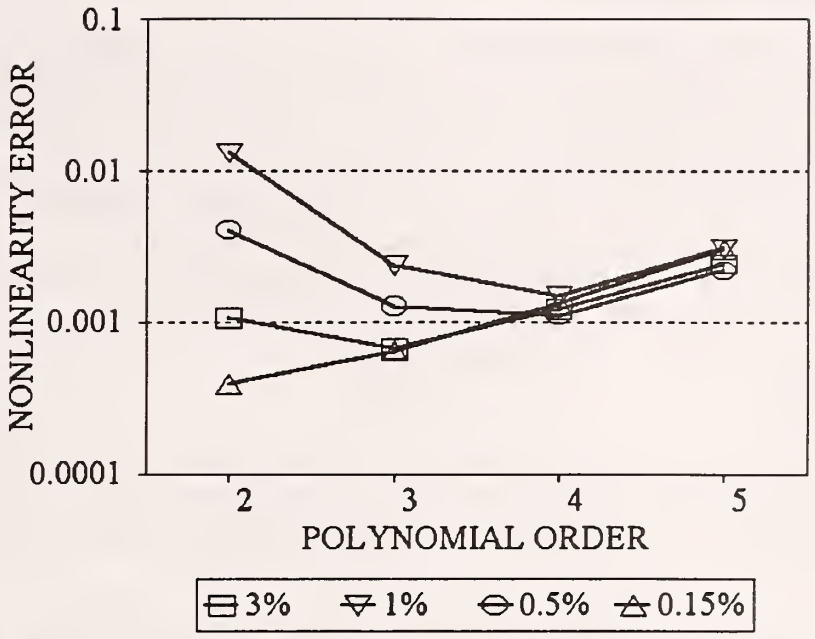

Figure 15. Combined error for four different response polynomials listed in table 3. This is the result for triplet method and the data random uncertainty is 0.01 percent.

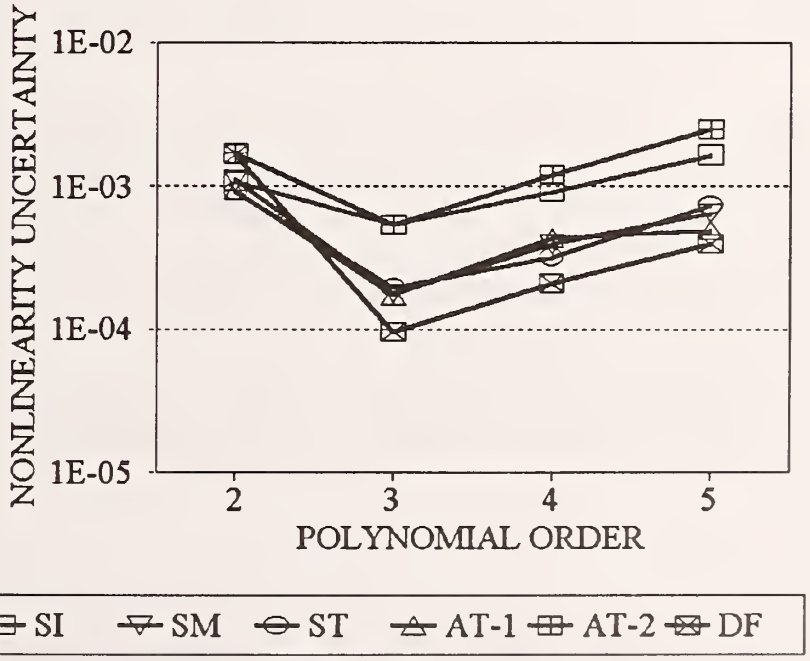

Figure 16. Combined nonlinearity uncertainty when data have the same 0.01 percent relative random uncertainty.

4.1.4. Effect of Reference Point

From section 2, we know that we can express the nonlinearity uncertainty with reference to any assumed calibration point without doing the calibration and later get the nonlinearity with reference to the real calibration point by eq (15). However, the standard deviation of the result using different dummy calibration points may not be the same. Figure 17 illustrates this effect of reference point for the triplet method. Since the data are taken between 0.1 and 1 times power interval, results using a reference point within that range have standard deviation significantly less than those with reference outside the data range. The best reference point is at the middle of the power range.

4.1.5. Other Results

Figure 18 demonstrates that, when the data have random uncertainty, increasing the number of data points will reduce the resultant uncertainty linearly by $\sqrt{N}$, where N is the number of data points. When the data are without uncertainty, increasing the number of data points will have small effect.

Figure 19 shows the uncertainty of transmittance (τ) obtained from the attenuation method by eq (34). One alternative way of using the attenuation method is to first measure the transmittance τ of the filter in the system. If we are able to make the positioning of the filter very repeatable, we can measure it many times, say 100 times, and obtain the magnitude of τ whose uncertainty is reduced to a tolerable level. Then we use this value of τ in the attenuation method. Figure 20 gives the effect of the deviation of the value of τ from the true value. We can determine from this figure what uncertainty is tolerable in the measurement of τ in order to achieve the target accuracy of the nonlinearity measurement.

We mentioned in the description of the differential method that the finite input of the ac signal will cause uncertainty in the result. Results of simulations of this effect are depicted in figure 21. When the ac input is one-hundredth of the maximum dc of the measurement range, the resulting systematic error and random uncertainty will almost be the same as those when we are measuring the true derivative of the conversion function, or when the ac input is 0. When the ac input is one-tenth of the maximum dc input, the uncertainties are noticeably different from the true derivative case. Because larger ac input means better signal-to-noise ratio in the ac measurement, a compromise must be made in the measurement between the extra uncertainty due to the finite ac input and the signal-to-noise ratio.

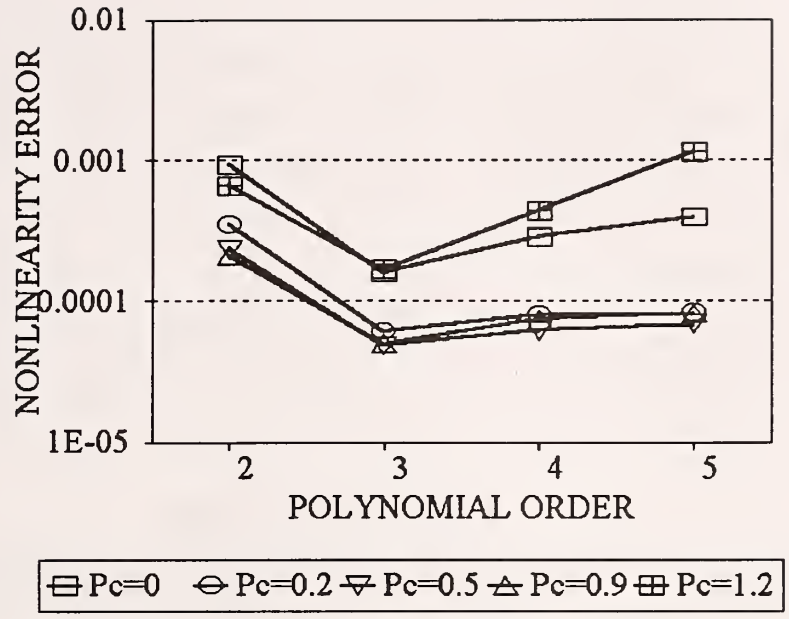

Figure 17. Nonlinearity error for different reference points for triplet superposition method.

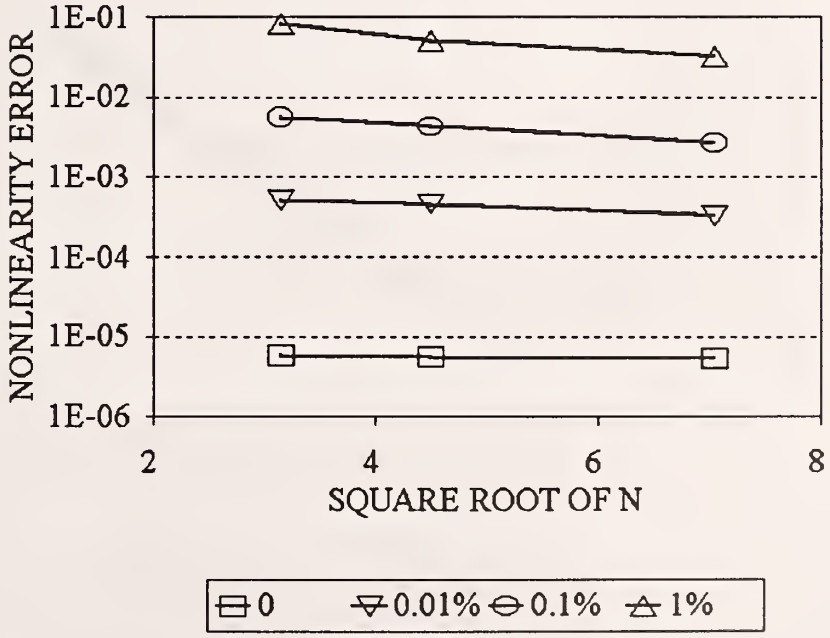

Figure 18. Nonlinearity error versus the square root of the number of data points.

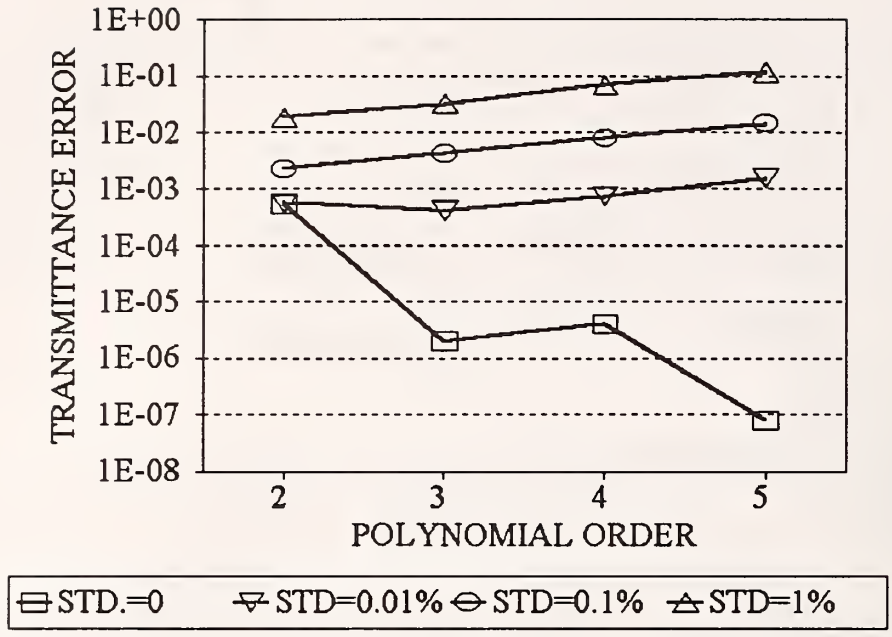

Figure 19. Error in the transmittance obtained from the attenuation method due to polynomial truncation and data random uncertainty.

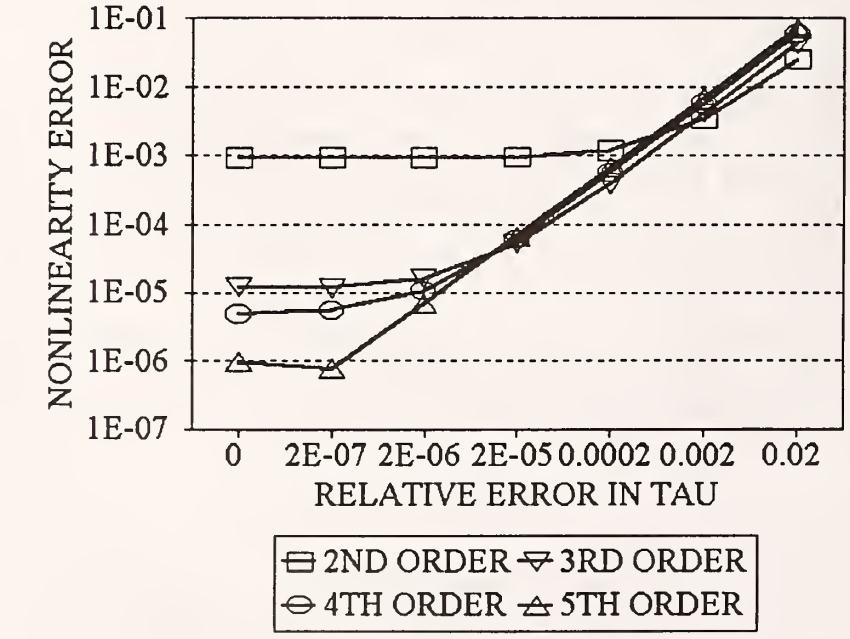

Figure 20. Nonlinearity error due to inaccurate transmittance used in the attenuation method.

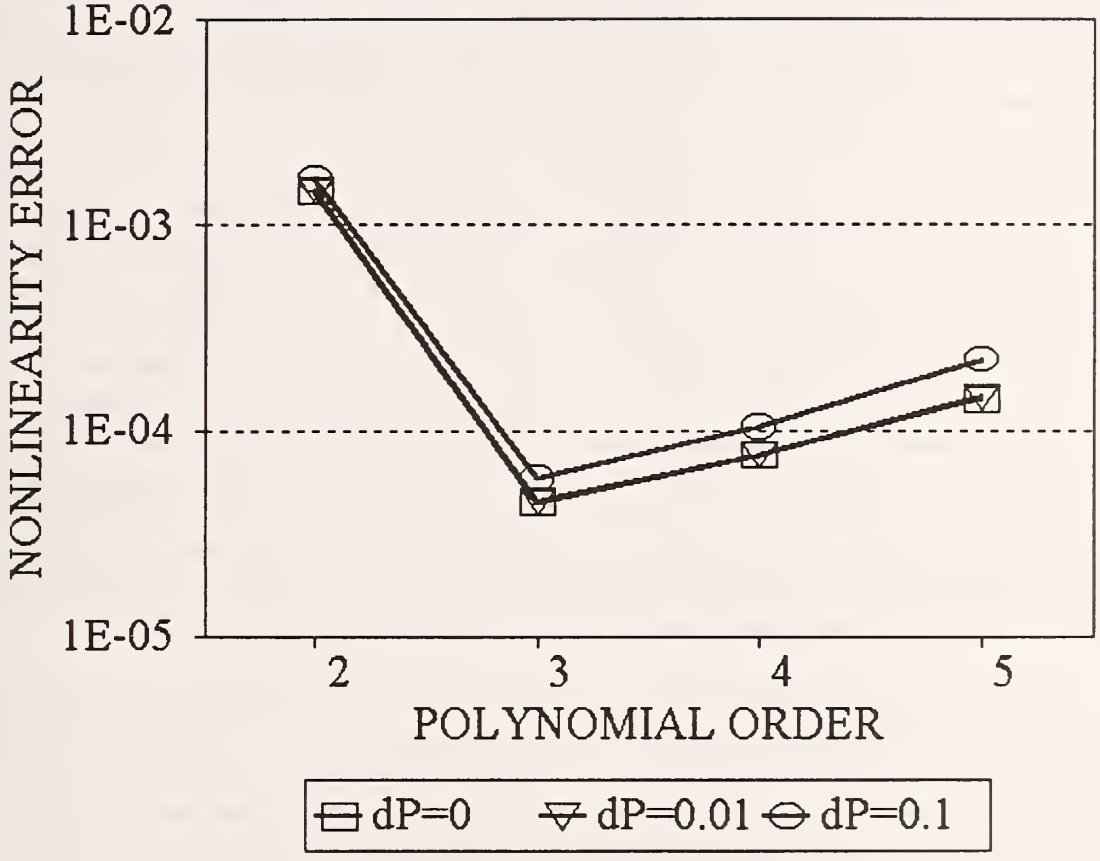

Figure 21. Nonlinearity error due to finite ac input in the differential method.

5. Conclusions

(1) A unified mathematical treatment has been established for all the measurement methods. Although detector nonlinearity is expressed with reference to the calibration point, it can be measured without first calibrating the detector. The nonlinearity is expressed with reference to any dummy calibration point which can later be converted to nonlinearity with reference to the real calibration point. A reference point at the middle of the measurement range is recommended, and reference points outside the data range should be avoided.

(2) Under the same conditions assumed in the simulations, all the superposition methods and the attenuation method, with the transmittance known accurately, yield the same accuracies, while the differential method shows a slightly higher systematic error and less random uncertainty than those methods. The attenuation method with unknown transmittance gives the largest systematic error and random uncertainty; the attenuation method with a known transmittance (with uncertainty) is not able to yield results as accurate as the superposition methods and the differential method. The integral-step superposition method has large random uncertainties in its results due to the accumulation of uncertainty in the data and consequently, requires a careful adjustment of the input power to avoid even higher uncertainties. Therefore, it is not a desirable choice. Because source drift may have a larger impact on the modified superposition method, we are left with the choice between the triplet superposition method and the differential method. However, the assumption of identical measurement conditions often does not hold for all these methods in a real measurement and it may be necessary to compare the methods under different conditions. Furthermore, effects other than those considered in our simulation may play an important role in determining the measurement accuracy. For example, attenuation method uses the simplest measurement setup, which will reduce the number of sources of potential uncertainty.

(3) The various methods have systematic errors and random uncertainties which behave differently depending on the fitting polynomial order. A compromise usually must be made. Because we can reduce the random uncertainty by increasing the number of data points and the number of measurements, keeping systematic errors well below the target accuracy usually is a priority. Systematic error depends very much on the real response function of the detector, which is not known. A fourth-order polynomial is recommended if the nonlinearity is very small (at or less than 0.1 percent) and the data standard deviation is very small (at or less than 0.05 percent). If the data standard deviation is not very small and the detector nonlinearity is at or above 1 percent, a third-order polynomial may be used. We suggest the following criterion when it is not obvious which polynomial order should be used. The same measurement data may be treated by both the third- and fourth-order polynomials. If the difference between the two results is less than the sum of the standard deviations of each of them, the two results are considered in agreement with each other statistically, and the third-order polynomial should be used. When the two results do not agree in this sense, truncation error may have caused the difference and therefore

the fourth-order polynomial should be used. If the system has large noise and nonlinearity, a fifth- or higher-order polynomial will yield a higher random uncertainty. Using too many data points or repetitions of measurements to reduce the random uncertainty is not always practical and may cause other technical problems; thus, fifth- or higher-order polynomials are not recommended unless the measurement system can produce data with extremely low random uncertainties and very small detector nonlinearities are to be measured.

This work is supported by the Calibration Coordination Group (CCG) of the Department of Defense with the lead agency for this project being the U.S. Naval Warfare Assessment Division, Corona, California. Matt Young, Robert Gallawa, and Steven Mechels of NIST reviewed the manuscript; the authors thank them for their comments.

6. References

[1] "Calibration of fiber-optic power meters," Draft International Standard, IEC TC 86, 1992.

[2] A.R. Schaefer, E.F. Zalewski, and Jon Geist, "Silicon detector nonlinearity and related effects, Appl. Opt. 22, 1232-1236 (1983).

[3] L. Coslovi and F. Righini, "Fast determination of the nonlinearity of photodetectors," Appl. Opt. 19, 3200-3203 (1980).

[4] R.D. Sanders and J.B. Schumaker, "Automated radiometric linearity tester," Appl. Opt. 23, 3504-3506 (1984).

[5] C.L. Sanders, "Accurate measurements of and corrections for nonlinearities in radiometers," J. Res. Nat. Bur. Stand. (U.S.) 76A, 437-453 (1972).

[6] H.J. Keegan, J.C. Schleter, and D.B. Judd, "Glass filters for checking performance of spectrophotometer-integrator systems of color measurements," J. Res. Nat. Bur. Stand. (U.S.) 66A, 203-221 (1962).

[7] D.E. Erminy, "Scheme for obtaining integral and fractional multiples of a given radiance," J. Opt. Soc. Amer. 53, 1448-1449 (1963).

[8] A. Reule, "Testing spectrophotometer linearity," Appl. Opt. 7, 1023-1028 (1968).

[9] H.J. Jung, "Spectral nonlinearity characteristics of low noise silicon detectors and their applications to accurate measurements of radiant flux ratios," Metrologia 15, 173-181 (1979).

[10] J. Fischer and L. Fu, "Photodiode nonlinearity measurement with an intensity stabilized laser as a radiation source," Appl. Opt. 32, 4187-4190 (1993).

[11] K.D. Mielenz and K.L. Ekerle, "Spectrophotometer linearity testing using double aperture method," Appl. Opt. 11, 2295-2303 (1972).

[12] W. Budde, "Multidecade linearity measurements on Si photodiodes," Appl. Opt. 18, 1555-1558 (1979).

[13] C.L. Sanders, "A photocell linearity tester," Appl. Opt. 1, 207-211 (1962).

[14] K.D. Stock, "Calibration of fiber optical power meters at PTB," Inst. Phys. Conf. Ser. No. 92, Int. Conf. Optical Radiometry, NPL, London, 12-13 April, 1988.

[15] R.G. Frehlich, "Estimation of the nonlinearity of a photodetector," Appl. Opt. 31, 5926-5929 (1992).

Appendix

We compare the variation of $\alpha = k\Delta P$ and $\left.\frac{dP(V)}{dV}\right|_{V=V_0}$ with the change of ΔP, where V_0 is the dc component of the ac output ΔV when the dc input $P = 0$. We can show immediately that

$$\frac{\delta\alpha}{\alpha} = \frac{\delta\Delta P}{\Delta P}. \tag{A1}$$

Denoting $\left.\frac{dP(V)}{dV}\right|_{V=V_0}$ as $P'(V_0)$, we have

$$dP'(V_0) = P''(V_0)dV_0, \tag{A2}$$

where $P''(V_0)$ is the second derivative of $P(V)$ at V_0. Then

$$\begin{aligned} \frac{dP'(V_0)}{P'(V_0)} &= \frac{P''(V_0)}{P'(V_0)}dV \\ &= \frac{P''(V_0)}{P'(V_0)}\left(\frac{dV}{dP}dP\right)\Big|_{V=V} \end{aligned} \tag{A3}$$

Using $P = P(V)$, we can further write

$$\frac{dP'(V_0)}{P'(V_0)} = \frac{P''(V_0)}{P'(V_0)}\frac{P(V_0)}{P'(V_0)}\left(\frac{dP}{P}\right)\Big|_{V=V_0} \tag{A4}$$

We denote $P = P_0$ when $V = V_0$. Because P_0 is the dc component of the ac input ΔP, it is proportional to the amplitude of the ac input ΔP and $d(\Delta P)/\Delta P = dP/P$. Thus we have

$$\frac{dP'(V_0)}{P'(V_0)} = \frac{P''(V_0)}{P'(V_0)}\frac{P(V_0)}{P'(V_0)}\left(\frac{d\Delta P}{\Delta P}\right)\Big|_{P=P_0} \tag{A5}$$

This result shows that the effect of the variation of input ac power is reduced (or magnified) by a factor of $\frac{P''(V_0)P(V_0)}{[P'(V_0)]^2}$. Using the normalized polynomial of eq (19) and the fact that nonlinearity is very small, we approximate this factor as

$$\sum_{k=2}^{n} b_k k(k-1)V_0^{k-1}.$$

Comparing this with eq (20), we can roughly estimate that

$$2\Delta_{NL}(V_0;0)\frac{dP_0}{P_0} < \frac{dP'(V_0)}{P'(V_0)} < 10\Delta_{NL}(V_0;0)\frac{dP_0}{P_0}. \tag{A6}$$

For small nonlinearity that is no more than a few percent, the effect of ac power drift is reduced at least by an order of magnitude.

*U.S. GOVERNMENT PRINTING OFFICE:1995-673-018/00106

NIST Technical Publications

Periodical

Journal of Research of the National Institute of Standards and Technology—Reports NIST research and development in those disciplines of the physical and engineering sciences in which the Institute is active. These include physics, chemistry, engineering, mathematics, and computer sciences. Papers cover a broad range of subjects, with major emphasis on measurement methodology and the basic technology underlying standardization. Also included from time to time are survey articles on topics closely related to the Institute's technical and scientific programs. Issued six times a year.

Nonperiodicals

Monographs—Major contributions to the technical literature on various subjects related to the Institute's scientific and technical activities.

Handbooks—Recommended codes of engineering and industrial practice (including safety codes) developed in cooperation with interested industries, professional organizations, and regulatory bodies.

Special Publications—Include proceedings of conferences sponsored by NIST, NIST annual reports, and other special publications appropriate to this grouping such as wall charts, pocket cards, and bibliographies.

Applied Mathematics Series—Mathematical tables, manuals, and studies of special interest to physicists, engineers, chemists, biologists, mathematicians, computer programmers, and others engaged in scientific and technical work.

National Standard Reference Data Series—Provides quantitative data on the physical and chemical properties of materials, compiled from the world's literature and critically evaluated. Developed under a worldwide program coordinated by NIST under the authority of the National Standard Data Act (Public Law 90-396). NOTE: The Journal of Physical and Chemical Reference Data (JPCRD) is published bi-monthly for NIST by the American Chemical Society (ACS) and the American Institute of Physics (AIP). Subscriptions, reprints, and supplements are available from ACS, 1155 Sixteenth St., NW, Washington, DC 20056.

Building Science Series—Disseminates technical information developed at the Institute on building materials, components, systems, and whole structures. The series presents research results, test methods, and performance criteria related to the structural and environmental functions and the durability and safety characteristics of building elements and systems.

Technical Notes—Studies or reports which are complete in themselves but restrictive in their treatment of a subject. Analogous to monographs but not so comprehensive in scope or definitive in treatment of the subject area. Often serve as a vehicle for final reports of work performed at NIST under the sponsorship of other government agencies.

Voluntary Product Standards—Developed under procedures published by the Department of Commerce in Part 10, Title 15, of the Code of Federal Regulations. The standards establish nationally recognized requirements for products, and provide all concerned interests with a basis for common understanding of the characteristics of the products. NIST administers this program in support of the efforts of private sector standardizing organizations.

Consumer Information Series—Practical information, based on NIST research and experience, covering areas of interest to the consumer. Easily understandable language and illustrations provide useful background knowledge for shopping in today's technological marketplace.
Order the **above** *NIST publications from: Superintendent of Documents, Government Printing Office, Washington, DC 20402.*
Order the **following** *NIST publications—FIPS and NISTIRs—from the National Technical Information Service, Springfield, VA 22161.*

Federal Information Processing Standards Publications (FIPS PUB)—Publications in this series collectively constitute the Federal Information Processing Standards Register. The Register serves as the official source of information in the Federal Government regarding standards issued by NIST pursuant to the Federal Property and Administrative Services Act of 1949 as amended, Public Law 89-306 (79 Stat. 1127), and as implemented by Executive Order 11717 (38 FR 12315, dated May 11, 1973) and Part 6 of Title 15 CFR (Code of Federal Regulations).

NIST Interagency Reports (NISTIR)—A special series of interim or final reports on work performed by NIST for outside sponsors (both government and non-government). In general, initial distribution is handled by the sponsor; public distribution is by the National Technical Information Service, Springfield, VA 22161, in paper copy or microfiche form.

U.S. Department of Commerce
National Institute of Standards and Technology
325 Broadway
Boulder, Colorado 80303-3328